Enhanced stimulated emission in ZnO thin films using microdisk top-down structuring

K. Nomenyo,[1] A.-S. Gadallah,[1,2] S. Kostcheev,[1] D. J. Rogers,[3] and G. Lérondel[1]
[1]*Laboratoire de Nanotechnologie et d'Instrumentation Optique, Institut Charles Delaunay, CNRS UMR 6281, Université de Technologie de Troyes, 12 rue Marie Curie, CS 42060, 10004 Troyes Cedex, France*
[2]*Department of Laser Sciences and Interactions, National Institute of Laser Enhanced Sciences, Cairo University, Giza, Egypt*
[3]*Nanovation, 8, route de Chevreuse, 78117 Châteaufort, France*

(Received 30 March 2014; accepted 21 April 2014; published online 8 May 2014)

Microdisks were fabricated in zinc oxide (ZnO) thin films using a top-down approach combining electron beam lithography and reactive ion etching. These microdisk structured thin films exhibit a stimulated surface emission between 3 and 7 times higher than that from a reference film depending on the excitation power density. Emission peak narrowing, reduction in lasing threshold and blue-shifting of the emission wavelength were observed along with enhancement in the emitted intensity. Results indicate that this enhancement is due to an increase in the internal quantum efficiency combined with an amplification of the stimulated emission. An analysis in terms of waveguiding is presented in order to explain these effects. These results demonstrate that very significant gains in emission can be obtained through conventional microstructuration without the need for more onerous top-down nanostructuration techniques. © *2014 AIP Publishing LLC*. [http://dx.doi.org/10.1063/1.4875744]

ZnO offers a combination of appealing attributes such as a direct wide bandgap, excellent temperature/radiation resistance, a tunable resistivity and good transparency right across the visible range plus low toxicity, a relatively high piezoelectric coefficient and a potential for optical emission with high quantum yields.[1,2] These properties predispose ZnO for a variety of applications such as low-threshold excitonic lasers (thanks to high optical gain and low loss, as recently reported by the authors[3]), UV photodetectors,[4] solar cells,[5] light emitting diodes,[6] and gas sensing.[7] Indeed, there has been a continuous exponential increase in reports on the manufacturing, characterization and applications of ZnO for a few decades now.[4,8]

Several different methods have been employed for the investigation of optically pumped ZnO lasing. Stimulated surface emission in ZnO thin films has been generated through scattering by surface undulations.[3,9,10] Stimulated edge emission has been produced by single pass gain in high quality thin films[3,10] or by coherent reflections from the facets of parallel hexagonal grains.[11] Stimulated edge emission has also been observed in random lasing mode for self-formed closed-loop reflections.[10]

Recently, there has been strong interest in generating ZnO lasing through nanosized or microsized whispering-gallery mode dielectric resonators.[12–17] Structures already reported deal with self-assembled microcavities, rather than etched thin films. One reason for this may be the difficulty in precise structuring of ZnO in a controlled manner by means of dry etching. However, microstructuration is usually significantly easier to realize than nanostructuration and thus appears a reasonable route to explore for applications in which stimulated surface emission is required such as third generation white LEDs (Light Emitting Diodes). This paper investigates the stimulated emission intensity and the lasing threshold for a top-down microdisk structuration of ZnO thin films. An analysis of the results in terms of waveguiding is also presented.

ZnO thin films were epitaxially grown on c-sapphire substrates by laser ablation of a 5N, sintered, ZnO target in a molecular oxygen ambient, as described elsewhere.[18] High resolution scanning electron microscopy (SEM) was conducted in a Raith e-line system. High resolution X-Ray Diffraction (XRD) was conducted in a Panalytical MRD (Materials Research Diffractometer) system. Stimulated emission was obtained by pumping with a frequency-tripled, Q-switched, Neodymium-doped Yttrium Aluminium Garnet (Nd:YAG) laser emitting at 355 nm (with 5 ns pulse duration and 10 Hz repetition rate). The focused pump laser beam was about 200 μm in diameter. The emission was collected from surface and end facets. Spectra were acquired using a standard photoluminescence set-up coupled to a spectrometer (50 cm focal length) with a Peltier-cooled charge coupled device camera. All measurements were carried out at room temperature. Ellipsometry was conducted in a Horiba UVISEL system.

Microdisk studies were conducted on a film which was found to have exceptional optical quality, with a gain higher than 1000 cm^{-1}, and scattering/absorption losses lower than 10 cm^{-1}.[3] The layer was estimated to be about 500 nm thick by ellipsometry. XRD revealed the film to be epitaxial with an omega rocking curve linewidth of 0.14° and a c lattice parameter of 5.209 Å, which is relatively close to the expected equilibrium value for wurtzite ZnO (about 5.206 Å). Thus, there was no indication of significant residual epitaxial strain at the film surface. Contact mode atomic force microscopy (AFM) revealed a root mean square roughness of about 2.5 nm with a peak-to-valley of 10 nm for a scan area of 2 μm × 2 μm. Four point measurements gave an average resistivity of about 0.3 Ω cm, which is typical for as-grown ZnO films, the film was subject to electron beam lithography (EBL) with a lift-off process after metal evaporation, as developed for the realization of plasmonic structures on glass substrates.[19] Subsequent mask transfer was achieved using

inductively coupled plasma (ICP) reactive ion etching (RIE). In the first attempt to realize ZnO mesostructures,[20] a metallisation of the poly-methyl methacrylate (PMMA) resist prior to exposure was used in order to avoid charging which results from the relatively low conductivity of the ZnO thin film. More precisely, the structuring process involved the cleaning of the ZnO thin film. Then a 160 nm thick PMMA layer was spin-coated on the sample and annealed at 160 °C for 3 h. The PMMA was then insolated using EBL. Before exposure, a 10 nm thick Al film was deposited on the annealed PMMA layer. The Al film was then chemically removed before the resist development. The EBL process was conducted at 10 kV and the dose was 100 μC/cm^2. After developing the PMMA resist, a 110 nm thick coating of Ni was evaporated onto the sample and a lift-off process was performed. In this way, ordered Ni microdisk masks were obtained on the ZnO surface. Finally, an RIE/ICP process was used to etch the ZnO through the mask, at a rate of 26 nm/s. Hexafluoroethane (C_2F_6) was used as the etching gas and the plasma was stabilized at 8 mTorr.[21]

A top-view electron micrograph of the etched ZnO microdisks is shown in Figure 1(a). Microdisks ranging in diameter from 0.5 μm to 6.5 μm were fabricated with a center-to-center distance of 10 μm. A side view micrograph, with a zoom-in on one of the microdisks is shown in Figure 1(b). Note that the thin film was not etched right down to the substrate. The total film thickness was about 564 nm, according to ellipsometry measurements, and the etched thickness was about 475 nm. The residual unetched ZnO thickness of 91 nm was left intentionally in order to reduce the loss of pump photons. Figures 2(a)–2(d) show the emission spectra for the thin film before (S1) and after (S2) the fabrication of microdisks. The diameter of the microdisks corresponding to these spectra was 3.5 μm. In order to appreciate the amplification effect, while keeping the spectra evolution visible, linear (Figures 2(a) and 2(b)) and logarithmic (Figures 2(c) and 2(d)) scales were used. For S1, below the stimulated emission threshold of about 2.7 MW/cm^2, the spectrum shows a weak band centered at around 383 nm. This band was attributed to radiative recombination of free excitons (P2 band).[9] Above the stimulated emission threshold, another intense and sharp peak emerges at about 395 nm. This peak was attributed to stimulated emission from an electron-hole plasma, or N-band.[22] With increasing incident intensity, the peak position showed a red-shift. This was attributed to bandgap renormalization.[23] The evolution from spontaneous emission to stimulated emission of S2 is similar to S1. The threshold for stimulated emission in S2 occurs at a lower value (2.25 MW/cm^2), however, and the emission intensity is higher than that of S1. This decrease in threshold was attributed to waveguiding within the microdisks by total internal reflection which increases nonlinear phenomena. In addition, the stimulated emission from the reference thin film (S1) is broader than that obtained from S2 and the emission peak is also red-shifted relative to that of S2. If a constant increase is observed for the plasma emission, the P2 emission is characterized by two distinct trends. First, an increase is observed below 5 MW/cm^2 and then the emission decreases. The use of microstructures in some specific excitation conditions reduces the amplified spontaneous emission (ASE) rate and the P2 emission intensity. These findings were attributed to a redistribution of the optical modes in the microstructured area.[24,25] As a consequence, the comparison study was limited to the plasma emission.

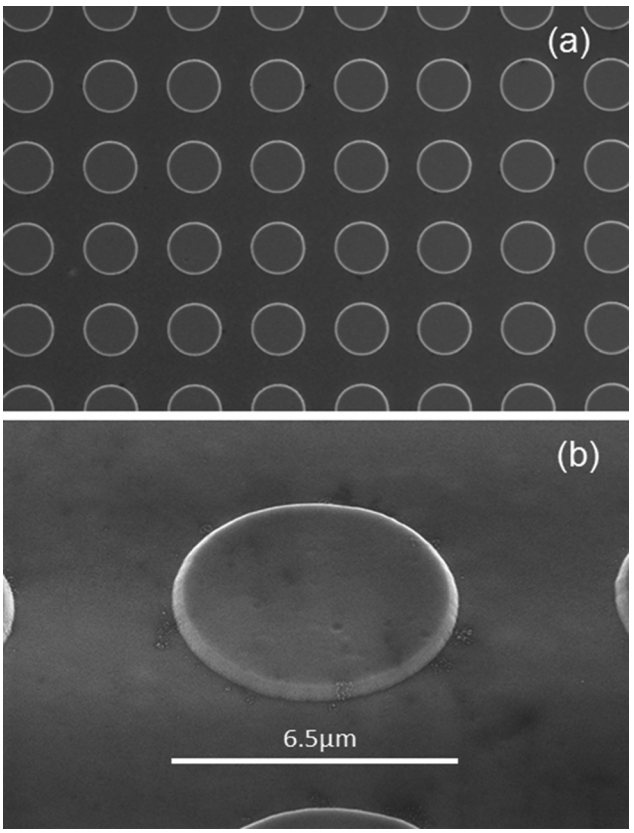

FIG. 1. (a) Top view electron micrograph of microdisks etched in a planar ZnO thin film, (b) Side view electron micrograph with zoom-in of a ZnO microdisk.

Figure 3(a) illustrates output-input intensity dependence for both S1 (circles) and S2 (squares) in a log-log scale. The emitted intensity for the microstructured thin film (S2) is higher than that for the reference (S1). Both samples, show a linear increase ($n = 5$) in plasma emission (confirming the plasma nature of the emission) plus a saturation regime ($n = 0.6$). At 1.38 MW/cm^2, S2 is already in the stimulated emission regime, whereas S1 is still in the ASE regime (dotted-line). In the plot of plasma emission evolution versus the excitation power density, a lasing threshold decrease is observed. This partially explains the enhanced stimulated emission. Indeed, the S2 curve in the $n = 5$ dependence range can be reproduced by horizontally translating (according to the a_1 vector) the emission curve for the S1 sample (dotted line). The stimulated emission enhancement in this range is due to the optical loss reduction as a result of the microdisk structuring. In order to fully overlap the two curves obtained for the S1 and S2 samples, vertical (b_2) and horizontal (a_2) translations are necessary. The vertical translation can be attributed to multiple reflexions within the microdisks. Figure 3(b) summarizes the different phenomena possible in the microstructured area: namely emission, waveguiding/multiple reflexions, reabsorption of photons and light extraction. In accordance with theoretical predictions, there is a 10% increase of the excitonic PL emission for both the S1

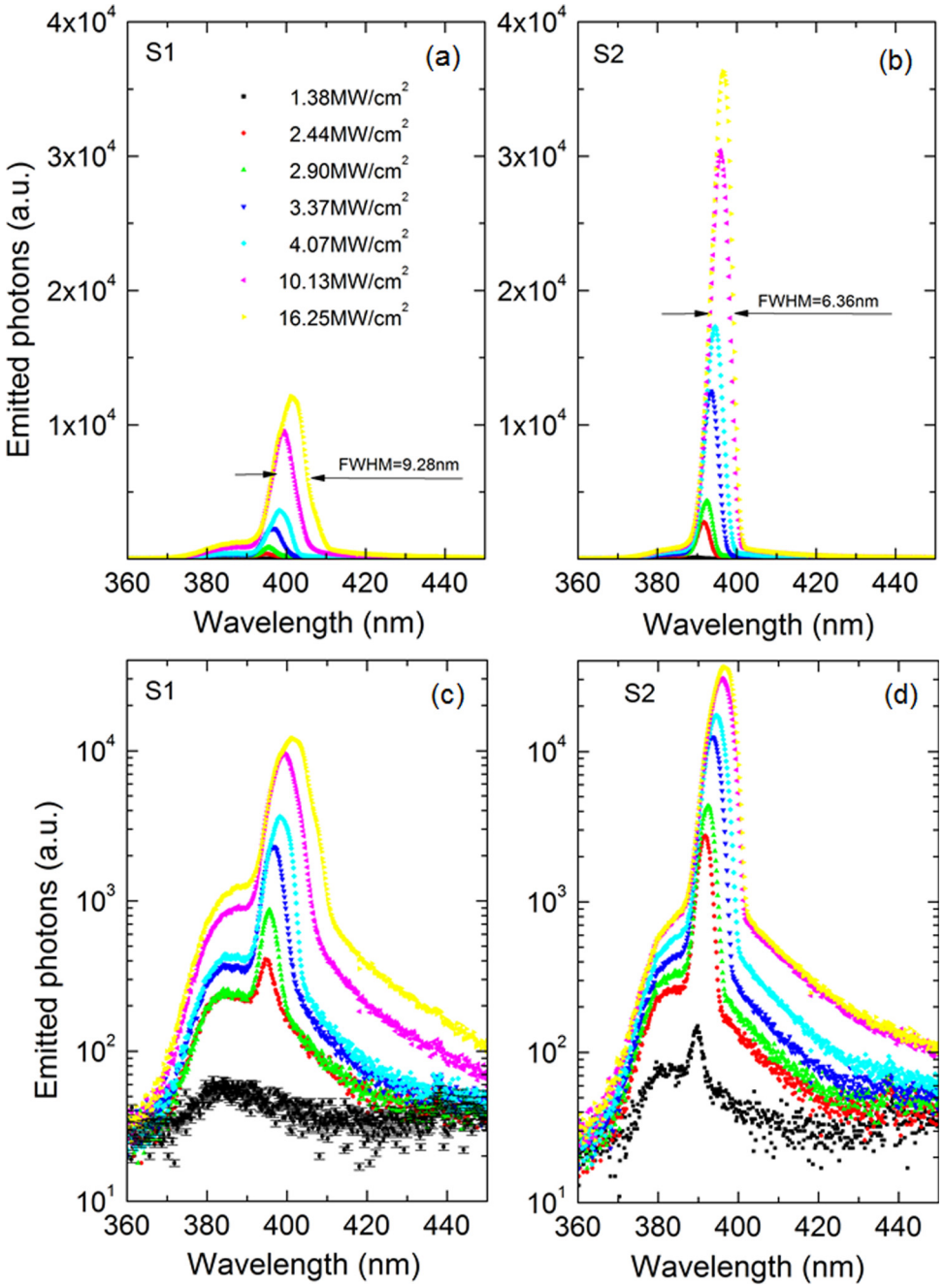

FIG. 2. Surface-emission spectra at different pumping intensities for a reference thin film, S1 and microdisk structured area S2 represented in linear (a) and (b) and log scale (c) and (d), respectively.

and S2 samples. This can be interpreted as the result of an increase in θ_c from 24° for S1 to $\theta_c + \Delta\theta < 30°$ for S2. These derivations show that light extraction is little affected by the structure geometry. Non-linear effects should, therefore, be taken into account. In the non-linear regime, the stimulated emission threshold strongly depends on the internal quantum efficiency (IQE). Considering N_{em} (the number of emitted photons) and N_{abs} (the number of absorbed photons) and assuming that N_{abs} is the sum of the lost photons (N_{los}) and the efficiently exciting photons (N_{exc}) the following relation is obtained for the IQE:

$$IQE = \frac{N_{em}}{N_{abs}} = \frac{N_{em}}{N_{los} + N_{exc}}. \quad (1)$$

The lower threshold observed in the case of the microstructured sample, S2, can be explain by an increase in the IQE, i.e., a decrease of N_{abs} as the result of a decrease in N_{los}. As a direct consequence of this, the amplification factor F (defined as follows) increases:

$$F = \frac{I_{EM}}{I_{ER}}, \quad (2)$$

where I_{EM} and I_{ER} are the emitted intensities of the plasma from the microdisk and the reference (above the stimulated emission thresholds), respectively. Figure 4(a) shows the enhancement factor, F, as a function of the incident intensity. A clear exponential decrease from 7 to 3 is observed as a

function of the excitation power. The maximum experimental F, of 7, is obtained before the saturation regime that finally leads to a 3.2 enhancement (F_0). The etching process employed to fabricate the microdisks produces a transverse refractive index gradient in the structure, since the refractive index in the ZnO microdisks (≈2 (Ref. 26)) is higher than that of the etched region between them. This transverse refractive index gradient produces optical waveguiding. Thus, the emission intensity is expected to be amplified due to an increase in the stimulated emission rate caused by the multiple reflection feedback loop. Peak narrowing was also observed to occur due to waveguiding and showed a dependence on the diameter of the microdisks. The full width at half maximum (FWHM) was about 9 nm for S1 and 6 nm for S2. For 5.5 μm diameter, it was further reduced to 3 nm. Thus the quality factor ($Q = \lambda/\Delta\lambda$) for the stimulated emission of the microstructured thin film was higher than for the reference film. Q was typically 126 for a 5.5 μm-diameter microdisk, 63 for a 3.5 μm-diameter microdisk and 46 for the reference film (S1). The blue shift for the microdisks, relative to S1, implies that there was a decrease in the effective refractive index of the microdisk structure compared to that for the reference film. Such a change in refractive index (Δn) can be estimated using the shift in the peak wavelength ($\Delta\lambda$ (nm)) through

$$\Delta n = \Delta\lambda \frac{n}{\lambda}, \tag{3}$$

where n is the refractive index of ZnO.

Figure 4(b) shows Δn (right axis) and $\Delta\lambda$ (left axis) as a function of the incident intensity. The negative value of $\Delta\lambda$ sign signifies the blue shift while the negative value of Δn signifies the decrease in the refractive index due to the formation of microdisks. The decrease in refractive index after the microdisk patterning also implies that there is a decrease in the reflectivity, R, at the air-semiconductor interface after etching. The pump intensity, I_p (MW/cm^2), is related to the incident intensity I_i (MW/cm^2) and R through

$$I_p = (1 - R)I_i. \tag{4}$$

Thus, the pump intensity for the microdisk is higher than of the reference film for the same incident intensity. The number of generated excitons per cubic centimeter, n_{ex}, is related to I_p through the following equation:[27]

$$n_{ex} = \frac{I_p \tau}{h\nu_p d}, \tag{5}$$

where τ is the exciton lifetime (taken to be 0.3 ns (Ref. 28)), $h\nu_p$ is the pump photon energy (J) and d is the film thickness (cm), respectively. Thus, the n_{ex} for the microdisk is higher than that for the reference film.

A similar trend was also observed for edge emission spectra obtained by transverse pumping using a cylindrical lens (results not shown). The film thickness in this case was 91 nm (bottom). The film was grown under the same conditions as S2. The F was than for the surface emission from the microdisks, however, the saturation value obtained for F, in case of stimulated edge emission, was 1.8. While the excitation

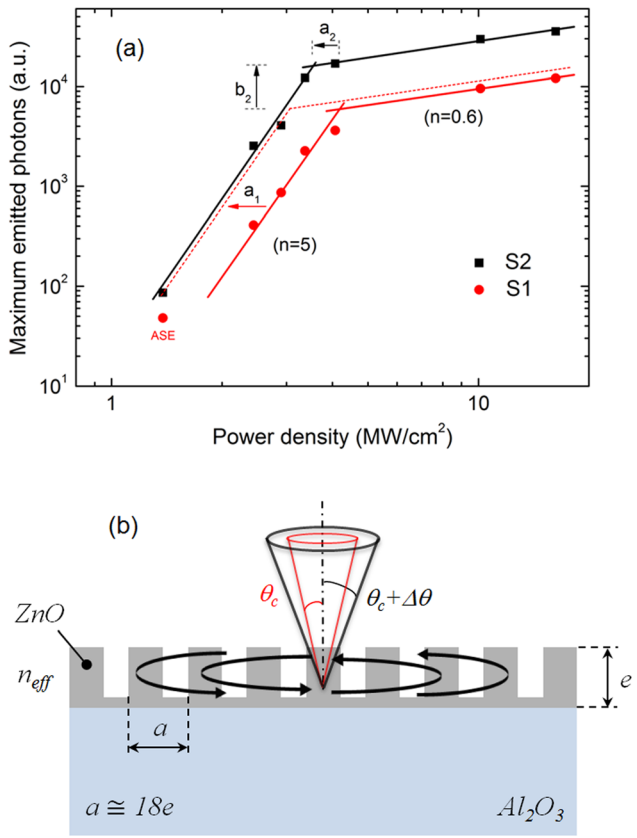

FIG. 3. (a) Maximum number of emitted photons as a function of the pumping power density in a log – log scale for the S1 (red) and S2 (black) samples. (N.B. The S2 curve (black) can be made to superimpose the S1 curve through simple horizontal and vertical translations). While the n = 5 dependence can be explained by a decrease of the lasing threshold, as shown by the red dotted line (horizontal translation by a1), the n = 0.6 dependence can only be explained by a change in the IQE of the stimulated emission. Fig. 3(b) summarizes the different phenomena at the origin of the stimulated emission enhancement in the microstructured area, namely waveguiding, multiple reflections, reabsorption of photons, and to some extent light extraction.

conditions were different and further modal analysis would be required,[29] these results indicate that the F factor for the microdisk structured thin film is higher and thus confirm the effect of the later for the stimulated emission efficiency. It should be noted, however, that the stimulated surface emission threshold (2.7 MW/cm^2) was higher than that for the stimulated edge emission (0.5 MW/cm^2). The lower threshold observed for the edge emission could be attributed to the different shape of the active medium.[3,10] As already explained for both surface and edge-emission (with a relatively small excitation area) the stimulated emission occurs through electron-hole plasma recombination and the emission is further amplified by either the increase of IQE (explained above), the single pass gain in an inverted region (stimulated edge-emission, as reported in Ref. 30), the scattering due to surface undulations (stimulated surface-emission, as reported in Ref. 9) or by waveguiding-assisted scattering due to surface undulations (stimulated surface-emission from the microdisks).

To conclude, top-down microstructured planar etched ZnO thin films with microdisks features were fabricated by combining EBL with a lift-off process after metal evaporation and RIE/ICP. An enhancement factor between 7 to 3

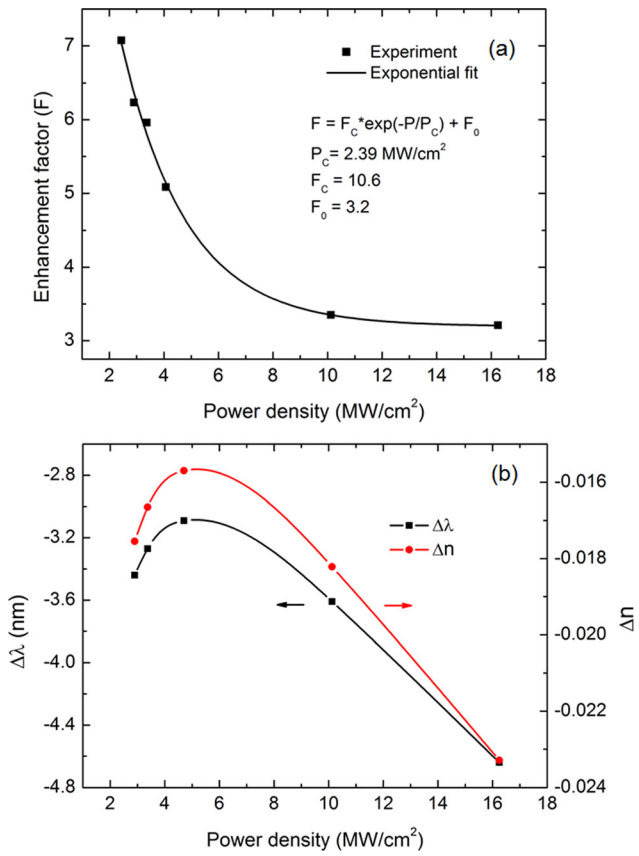

FIG. 4. (a) Enhancement factor, F, as a function of the pump power density. Fig. (b) Peak wavelength change (left axis) and change in effective refractive index (right axis) versus the incident power density for the ZnO microdisks area.

times higher than the reference film was obtained, depending on the excitation power density. Threshold reduction, IQE increase, emission peak narrowing and blue-shifting of the stimulated emission, were also observed and analyzed in terms of waveguiding. These results confirm the significance of top-down microdisk structuring for ZnO thin films and their potential for use in next-generation UV photonic devices.

This work was supported by the CPER MATISSE project. A.G. would like to thank Campus France and K.N. acknowledges the financial support of the "Champagne-Ardennes" region and the European Social Fund (FEDER).

[1]Ü. Özgür, Ya. I. Alivov, C. Liu, A. Teke, M. A. Reshchikov, S. Doğan, V. Avrutin, S.-J. Cho, and H. Morkoç, J. Appl. Phys. **98**, 041301 (2005).
[2]S. Xu and Z. L. Wang, Nano Res. **4**(11), 1013–1098 (2011).
[3]A.-S. Gadallah, K. Nomenyo, C. Couteau, D. J. Rogers, and G. Lérondel, Appl. Phys. Lett. **102**, 171105 (2013).
[4]D. J. Rogers, P. Bove, E. V. Sandana, M. Razeghi and F. H. Teherani, Laser Focus World, (2013), p. 49.
[5]Y.-H. Lin, P.-C. Yang, J.-S. Huang, G.-D. Huang, I.-J. Wang, W.-H. Wu, M.-Y. Lin, W.-F. Su, and C.-F. Lin, Sol. Energy Mater. Sol. Cells **95**, 2511 (2011).
[6]Y.-S. Choi, J.-W. Kang, D.-K. Hwang, and S.-J. Park, IEEE Trans. Electron Devices **57**(1), 26 (2010).
[7]S. S. Badadhe and I. S. Mulla, Sens. Actuators, B **156**, 943 (2011).
[8]Ü. Özgür, D. Hofstetter, and H. Morkoc, Proc. IEEE **98**, 1255 (2010).
[9]X. Q. Zhang, I. Suemune, H. Kumano, J. Wang, and S. H. Huang, J. Appl. Phys. **96**, 3733 (2004).
[10]P.-H. Dupont, C. Couteau, D. J. Rogers, F. Hosseini-Téhérani, and G. Lérondel, Appl. Phys. Lett. **97**, 261109 (2010).
[11]Z. K. Tang, M. Kawasaki, A. Ohtomo, H. Koinuma, and Y. Segawa, J. Cryst. Growth **287**, 169 (2006).
[12]T. Nobis, E. M. Kaidashev, A. Rahm, M. Lorenz, and M. Grundmann, Phys. Rev. Lett. **93**, 103903 (2004).
[13]C. Czekalla, C. Sturm, R. Schmidt-Grund, B. Cao, M. Lorenz, and M. Grundmann, Appl. Phys. Lett. **92**, 241102 (2008).
[14]R. Chen, B. Ling, X. W. Sun, and H. D. Sun, Adv. Mater. **23**, 2199–2204 (2011).
[15]J. Wiersig, Phys. Rev. A **67**, 023807 (2003).
[16]M. Willander, M. Q. Israr, J. R. Sadaf, and O. Nur, Nanophotonics **1**, 99 (2012).
[17]S. M. Spillane, T. J. Kippenberg, and K. J. Vahala, Nature (London) **415**, 621 (2002).
[18]D. J. Rogers, F. H. Teherani, A. Yasan, R. McClintock, K. Mayes, S. R. Darvish, P. Kung, M. Razeghi, and G. Garry, Proc. SPIE **5732**, 412 (2005).
[19]G. Lérondel, S. Kostcheev and J. Plain, "Nanofabrication for plasmonics," in *Plasmonics*, Springer Series in Optical Sciences Vol. 167 (2012), p. 269.
[20]L. Divay, D. J. Rogers, A. Lusson, S. Kostcheev, S. Mc Murtry, G. Lérondel and F. Hosseini-Téhérani, Phys. Status Solidi C **5**, 3095 (2008).
[21]D. Y. Lee and C. W. Chung, Thin Solid Films **518**, 372 (2009).
[22]P. Zu, Z. K. Tang, G. K. L. Wong, M. Kawasaki, A. Ohtomo, H. Koinuma, and Y. Segawa, Solid State Commun. **103**, 459 (1997).
[23]D. M. Bagnall, Y. F. Chen, Z. Zhu, T. Yao, M. Y. Shen, and T. Goto, Appl. Phys. Lett. **73**, 1038 (1998).
[24]M. Fujita, S. Takahashi, Y. Tanaka, T. Asano, and S. Noda, Science **308**(5726), 1296–1298 (2005).
[25]T. Baba and D. Sano, IEEE J. Sel. Top. Quantum Electron. **9**(5), 1340 (2003).
[26]Y. S. Park and J. R. Schneider, J. Appl. Phys. **39**, 3049 (1968).
[27]C. Klingshirn, R. Hauschild, J. Fallert, and H. Kalt, Phys. Rev. B **75**, 115203 (2007).
[28]M. H. Haung, S. Mao, H. Feik, H. Yan, Y. Wu, H. Kind, E. Weber, R. Russo, and P. Yang, Science **292**, 1897 (2001).
[29]R. Aad, L. Divay, A. Bruyant, S. Blaize, C. Couteau, D. J. Rogers, and G. Lerondel, J. Appl. Phys. **112**, 063112 (2012).
[30]C. Czekalla, J. Lenzner, A. Rahm, T. Nobis, and M. Grundman, Superlattices and Microstructures **41**, 347 (2007).